

CrystEngComm

Accepted Manuscript



This is an *Accepted Manuscript*, which has been through the Royal Society of Chemistry peer review process and has been accepted for publication.

Accepted Manuscripts are published online shortly after acceptance, before technical editing, formatting and proof reading. Using this free service, authors can make their results available to the community, in citable form, before we publish the edited article. We will replace this *Accepted Manuscript* with the edited and formatted *Advance Article* as soon as it is available.

You can find more information about *Accepted Manuscripts* in the [Information for Authors](#).

Please note that technical editing may introduce minor changes to the text and/or graphics, which may alter content. The journal's standard [Terms & Conditions](#) and the [Ethical guidelines](#) still apply. In no event shall the Royal Society of Chemistry be held responsible for any errors or omissions in this *Accepted Manuscript* or any consequences arising from the use of any information it contains.

IR Spectroscopy as a probe for C–H \cdots X hydrogen bonded supramolecular synthons

Subhankar Saha, Lalit Rajput, Sumy Joseph, Manish Kumar Mishra, Somnath Ganguly* and Gautam R. Desiraju*

Solid State and Structural Chemistry Unit, Indian Institute of Science, Bangalore 560 012, India.

E-mail: desiraju@sscu.iisc.ernet.in

Abstract:

Weak hydrogen bonds of the type C–H \cdots X (X: N, O, S and halogens) have evoked considerable interest over the years, especially in the context of crystal engineering. However, association patterns of weak hydrogen bonds are generally difficult to characterize, and yet the identification of such patterns is of interest, especially in high throughput work, or where single crystal X-ray analysis is difficult or impossible. To obtain structural information on such assemblies, we describe here a five step IR spectroscopic method that identifies supramolecular synthons in weak hydrogen bonded dimer assemblies, bifurcated system, and π -electron mediated synthons. The synthons studied here contain C–H groups as hydrogen bond donors. The method involves (i) identification of simple compounds/cocrystals/salts that contain the hydrogen bonded dimer synthon of interest or linear hydrogen bonded assemblies between the same functionalities; (ii) scanning infrared (IR) spectra of the compounds; (iii) identifying characteristic spectral differences between the dimer and linear and; (iv) assigning identified bands as marker bands for identifying the supramolecular synthon, and finally (v) identifying synthons in compounds whose crystal structures are not known. The method has been effectively implemented for assemblies involving dimer/linear weak hydrogen bonds in nitrobenzenes (C–H \cdots O–NO), nitro-dimethylamino compounds (NMe₂ \cdots O₂N), chalcones (C–H \cdots O=C), benzonitriles (C–H \cdots N \equiv C)

and fluorobenzoic acids ($C-H \cdots F-C$). Two other special cases of $C-H \cdots \pi$ and $N-H \cdots \pi$ synthons were studied in which the band shape of the C–H stretch in hydrocarbons and the N–H deformation in aminobenzenes was examined.

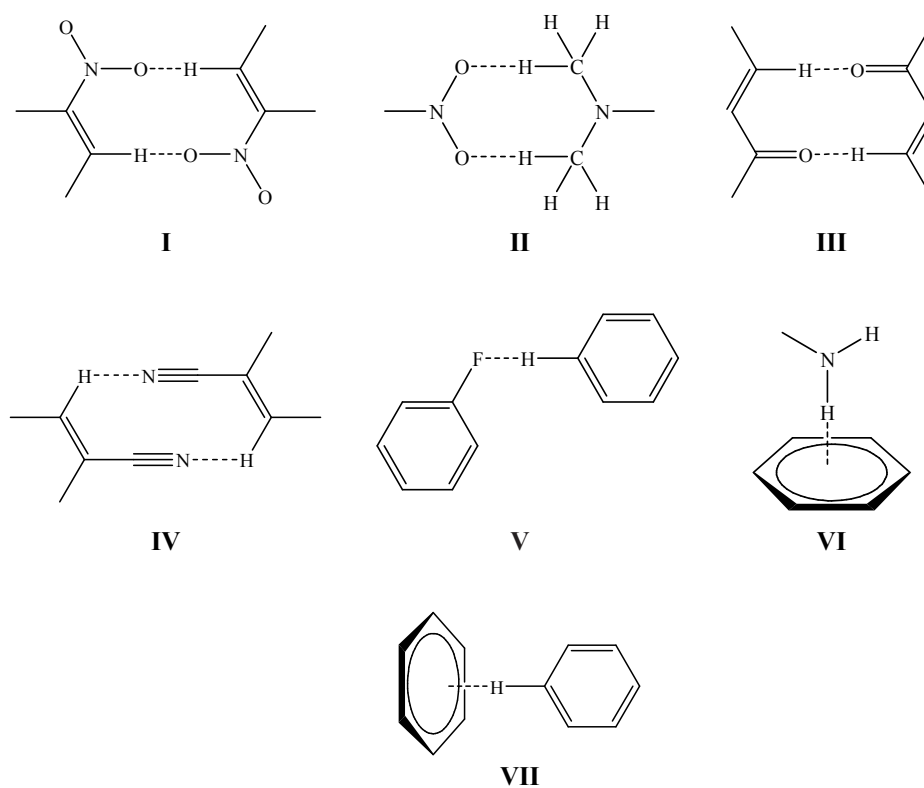
Introduction

Supramolecular synthons are structural units that contain geometrical and chemical information required for recognition between functional groups in molecular solids.^{1,2} Homosynthons and heterosynthons have acquired significance due to the relevance of cocrystals that have applications in fields ranging from drug design (structure–activity relationships) to organic electronics.³⁻⁹ Weaker hydrogen bonds of the type C–H···X (X: N, O, S and halogens) as defined by Desiraju and Steiner and synthons formed by them are of considerable interest.¹⁰ Although these interactions have energies only in the range 2–20 kJmol⁻¹, their effects on crystal structure and packing are just about as relevant as are the effects of conventional hydrogen bonded systems.^{11,12} Weak hydrogen bonds play distinctive roles in molecular recognition,¹³ guiding molecular association,¹⁴ and shaping molecular and supramolecular architectures.¹⁵ The relevant compound classes include organic and bio-organic systems, advanced organic materials and also DNA and proteins.¹⁶ Because of the weakness of these interactions, their analysis in terms of crystallographic, spectroscopic, and computational methods is both subtle and implicit. Furthermore, it may not always be possible to employ conventional SCXRD methods to elucidate structural information when single crystals are difficult to grow or if the analysis is of a high throughput type. In these situations, crystal structure prediction (CSP) technique is successful up to a certain extent.¹⁷ However, CSP has its own limitations such as too many possible conformations for a particular molecule or several functional groups involved with the complex molecular association patterns.¹⁸ Supramolecular synthon-based CSP is a promising strategy in this overall attempt.¹⁹ In general, however, there is a need to obtain basic synthon information in polycrystalline samples. Powder XRD (PXRD) is helpful in providing the bulk phase purity, but it cannot be applied for routine synthon identification. A simple, robust, and

accurate method that can identify supramolecular synthons is of significance especially in high throughput screening. IR or Raman methods could offer a solution provided bands or band-sets can be identified for a particular supramolecular synthon.^{20, 21} Here, we have attempted to extend our IR method of characterizing synthons to structural units that incorporate weak hydrogen bonds. Our method uses IR marker bands. The formation of a dimer hydrogen bond of C–H···X type assembly can be probed by IR spectroscopy. The present approach towards elucidation of weakly hydrogen bonded dimer synthons involves identifying compounds that exhibit positional isomerism as for example the nitrobenzenes, nitro-dimethylamino compounds, chalcones, benzonitriles, and fluorobenzoic acids. These compounds can form dimer synthons with C–H···O–NO, C–H···O=C, or C–H···N type hydrogen bonds in certain substitutions while in other substitutions of the same molecule, linear synthons of the molecular assembly may be seen. In the case of fluorobenzoic acids there is a possibility of bifurcation in the C–H···F–C hydrogen bonds which can be probed by IR. We have recently employed IR spectroscopy to identify strong hydrogen bonded and halogen bonded synthons.²⁰ However, to our knowledge, an IR method of identifying weakly hydrogen bonded dimer synthons that can differentiate the linear weak hydrogen bonded assembly has not been attempted previously and will be useful where there are problems with traditional single crystal X-ray diffraction (SCXRD) methods.

The C–H stretch is an anharmonic vibration and it leads to coupling of the stretching vibrations with overtones and summation frequencies of modes in the medium frequency range below 1800 cm^{-1} , particularly the $\delta(\text{C–H}\cdots\text{X})$ and $\gamma(\text{C–H}\cdots\text{X})$ protonic deformation (out of plane and in plane) vibrations.^{22, 23} When there is a formation of dimer-like structure containing a C–H···X bond, this perturbs the hydrogen bonded C–H stretching vibration leading to distinct changes in the C–H band structure as well as frequency and this causes further changes in the

medium frequency vibrations, particularly to the $\delta(\text{C-H}\cdots\text{X})$ and $\gamma(\text{C-H}\cdots\text{X})$ deformation vibrations. The resultant stretching/deformation bands can be used as marker bands of the dimer. This unique approach can differentiate the weak hydrogen bonded dimer from the linear within the same functional groups. Groups that are attached to the dimer arms are expected to be perturbed during dimer formation and such functional groups are also monitored in some cases to probe dimer formation.



Scheme 1: Supramolecular synthons in the present IR study.

Results and discussion:

Method:

In the present study, we have selected few model compounds with known crystal structures involving weak hydrogen bonded synthons (Scheme 1). The assemblies representing the dimer/ linear structures are C–H \cdots O–NO hydrogen bond in the nitrobenzenes, NMe₂ \cdots O₂N in nitro-dimethylamino compounds, C–H \cdots O=C hydrogen bond in chalcones, C–H \cdots N \equiv C in the benzonitriles, and C–H \cdots F–C synthon in fluorobenzoic acids. In some cases dimers are associated with typical C–H stretching and bending vibrations which are different from the linear hydrogen bond vibrations. In the case of C–H \cdots O involving the nitro functionality, the asymmetric and symmetric stretch, and scissoring/wagging bending modes of the nitro group were monitored for the presence of dimer.²⁴ Similarly in the C–H \cdots N dimer the asymmetric C–H stretch was analyzed for identification of the dimer.²⁵ By monitoring the vibrational spectra one can identify typical dimer vibrations and hence confirm the presence or absence of the dimer synthon. Further, two other special cases of the C–H \cdots π and N–H \cdots π synthons are studied by examining the band shapes of the C–H and N–H stretching/bending absorptions respectively in the aromatic hydrocarbons and aminobenzenes respectively.

The five step process:

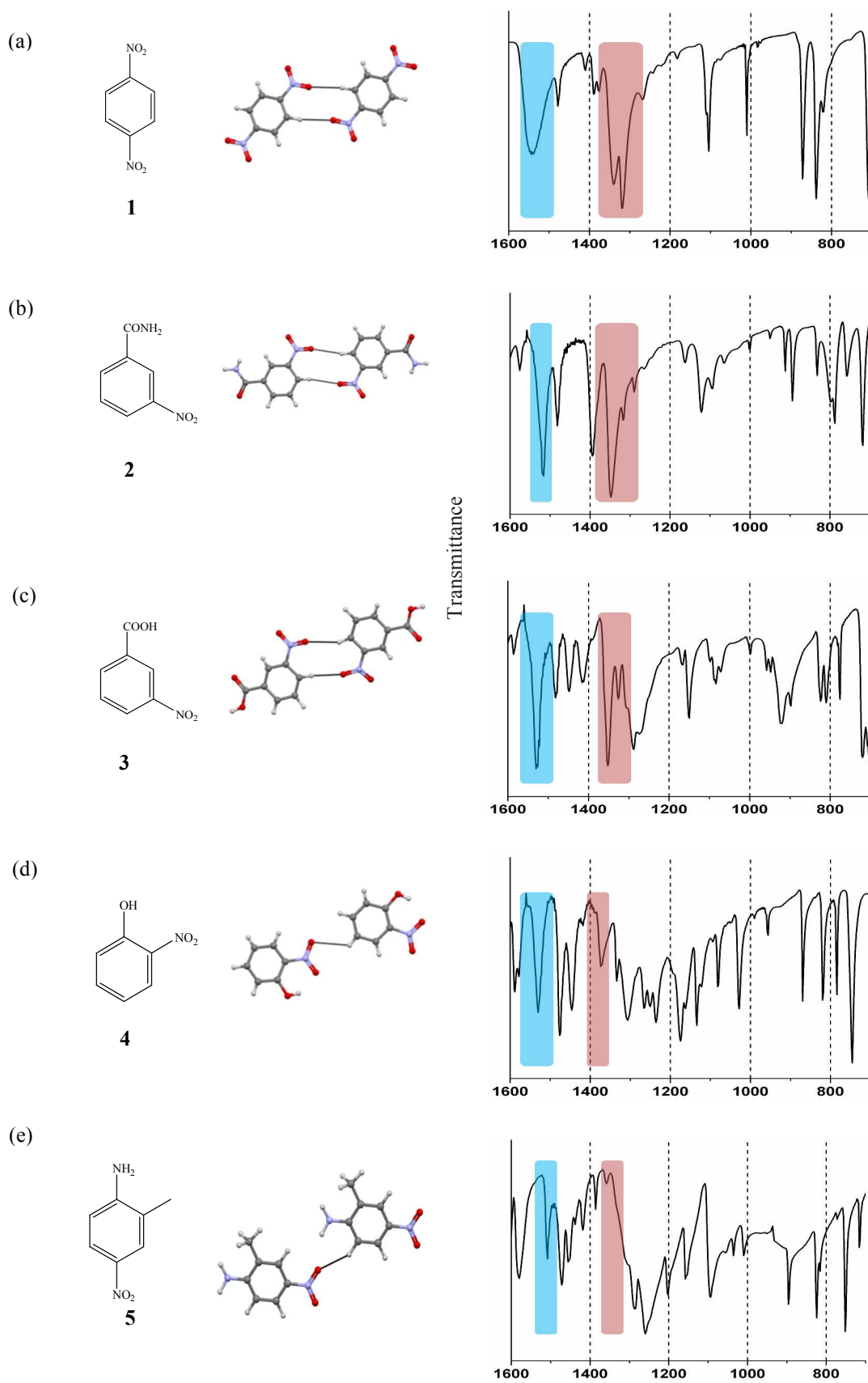
1. Identification of compounds that contains the *dimer* synthon / *linear* hydrogen bond between the same functional groups whose SCXRD is reported.
2. Recording the FTIR spectra of the compounds identified in (1).
3. Noting the differences in the IR bands for the dimer and the linear non-covalent interactions and identifying such differences as marker bands of the dimer synthon.
4. Vibrational assignment of marker bands of the *dimer*.

5. Identification of dimer synthon in unknown (whose SCXRD is not reported) compounds.

This five step process was applied to the compounds involving synthons **I** to **IV** to identify the IR marker bands for dimers. In case of synthon **V**, the effect of bifurcation has been identified in some well known fluorobenzoic acids. Synthons **VI** and **VII** involving π -electrons have been analyzed by monitoring the band shapes. Each synthon is investigated individually and discussed in detail below.

C–H \cdots O–NO dimer synthon:

For the studies of the centrosymmetric dimer synthon **I**, we have selected compounds **1-3** having dimer, and **4-5** with linear C–H \cdots O–NO hydrogen bond. FTIR spectra of the compounds were scanned (Fig. 1). The crystal structures of compounds **1-5** are reported. The synthon **I** dimer is characterized by the appearance of a strong split of the symmetric NO₂ stretch (ν_s) at ~ 1350 cm⁻¹ (Table 1).²⁶ The splitting of the symmetric stretch is clear and the band has intensity greater or comparable with respect to the asymmetric stretch (ν_{as}) which appears at ~ 1530 cm⁻¹. In the spectrum of **4** and **5** having a linear C–H \cdots O–NO hydrogen bond, the IR spectrum shows a completely different character for the N–O vibrations: the asymmetric stretching band has intensity higher than the symmetric stretching absorption, without the characteristic splitting (Fig. 1d).²⁷ The splitting and intensity increase of the symmetric stretch of NO₂ group may be due to different bonding environments of two N–O bonds in the synthon, clearly indicating a dimer-like structure.^{28, 29}



Wavenumber (cm⁻¹)

Fig. 1. Compounds (a) **1**, (b) **2**, and (c) **3** with dimer synthon **I** and (d) **4**, (e) **5** with linear hydrogen bond, and the IR spectra.

Table 1: IR characteristics of compounds 1-5.

Compounds	Synthon	NO ₂ ν_{as} ^A band (cm ⁻¹)	NO ₂ ν_s ^B band (cm ⁻¹)	I_{as} vs I_s ^C	Splitting at ν_s (cm ⁻¹)
1	Dimer	1540	1340	$I_{as} < I_s$	22
2	Dimer	1516	1348	$I_{as} < I_s$	30
3	Dimer	1530	1352	$I_{as} \sim I_s$	26
4	Linear	1530	1374	$I_{as} > I_s$	-
5	Linear	1508	1357	$I_{as} > I_s$	-

^ANO₂ asymmetric stretching band, ^BNO₂ symmetric stretching band, and ^C I_{as} : Intensity of NO₂ ν_{as} band, and I_s : Intensity of NO₂ ν_s band.

Once the characteristics of the dimer and linear synthons are identified, this information can be used to identify the presence or absence of a dimer in an unknown compound. We have chosen two unknown compounds **6** and **7** whose crystal structures are not reported (Fig. 2). The IR spectra of both compounds were recorded. When the spectra mapped with the identified markers, it was clearly seen that compound **6** exhibits a dimer synthon while compound **7** is a linear (Table 2).

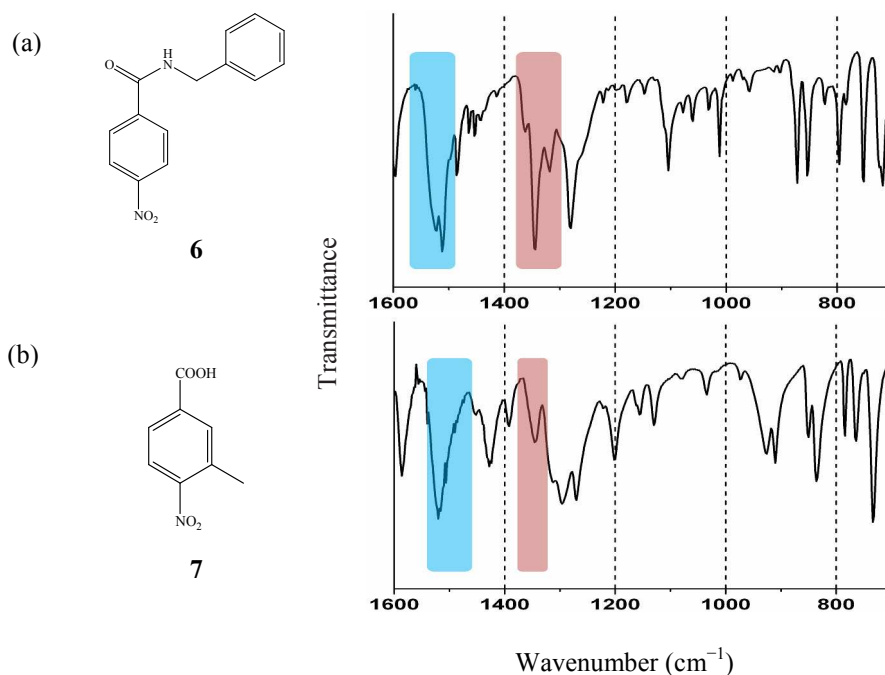


Fig. 2: IR spectra of (a) **6** and (b) **7**.

Table 2: IR characteristics of compounds **6** and **7**.

Compounds	NO ₂ ν_{as} ^A band (cm ⁻¹)	NO ₂ ν_s ^B band (cm ⁻¹)	I_{as} vs I_s ^C	Splitting at ν_s (cm ⁻¹)	Conclusion
6	1524	1344	$I_{as} < I_s$	26	Dimer
7	1520	1346	$I_{as} > I_s$	-	Linear

^ANO₂ asymmetric stretching band, ^BNO₂ symmetric stretching band, and ^C I_{as} : Intensity of NO₂ ν_{as} band, and I_s : Intensity of NO₂ ν_s band.

The synthons were confirmed by SCXRD (Fig. 3). SCXRD reveals that compound **6** has a dimer synthon **I** at a distance (vdW+0.2) Å whereas **7** exhibits a linear C–H⋯O–NO hydrogen bond. The crystal structure information validates the process of the present IR study.

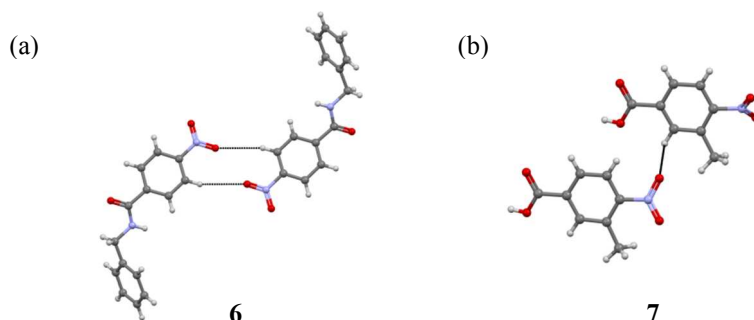
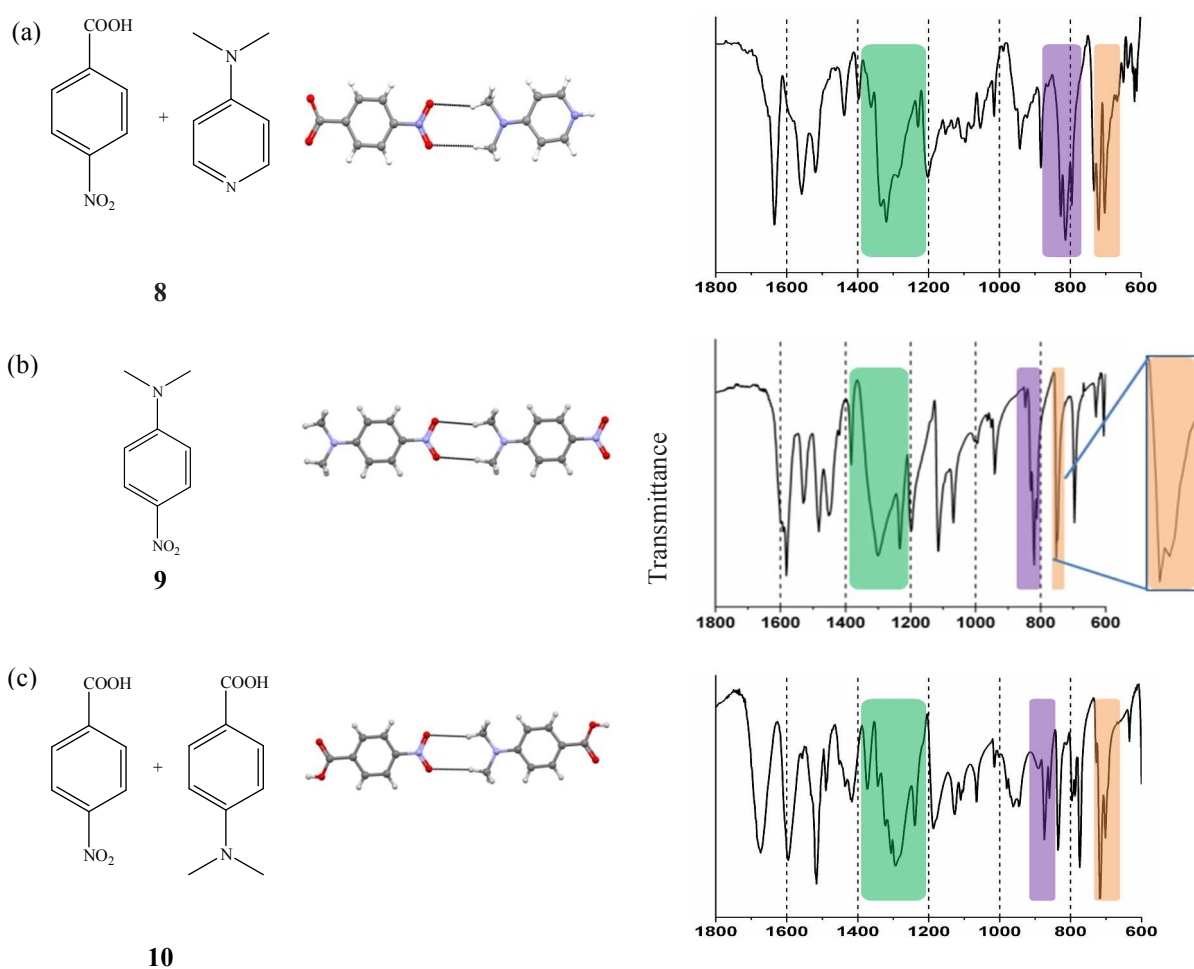


Fig. 3: Crystal structures of compound (a) **6** (exhibit synthon-I) and (b) **7** (exhibit linear C–H⋯O–NO hydrogen bond).

NMe₂⋯O₂N dimer synthon:

For the study of synthon **II** (NMe₂⋯O₂N dimer), we selected compounds **8-12** whose crystal structures are reported (Fig. 4). Compounds **8-10** have the dimer whereas **11-12** are linear. FTIR spectra of the compounds were scanned. The dimer is characterized by the appearance of a strong and unusually broad symmetric NO₂ stretch (ν_s) with bands appearing at ~1330 cm⁻¹(Table 3).²⁶ In contrast, linear **10-12** have sharp ν_s band. The IR analysis also shows the

splitting of NO₂ scissoring, and NO₂ wagging mode in cases of the dimers which is absent for the linear. Coupling of vibrations are well known in dimer structures and lead to changes in the structure and breadth of the stretching and bending modes.^{30, 31} In the dimer NMe₂⋯O₂N synthon a coupling of the methyl vibrations and the symmetric NO₂ that occur in close proximity is the reason for the unusual width of the band at ~1330 cm⁻¹. These IR features, (i) broad NO₂ ν_s band, (ii) split NO₂ scissoring mode, and (iii) NO₂ wagging mode can be used to identify the presence of dimer synthon **II**.



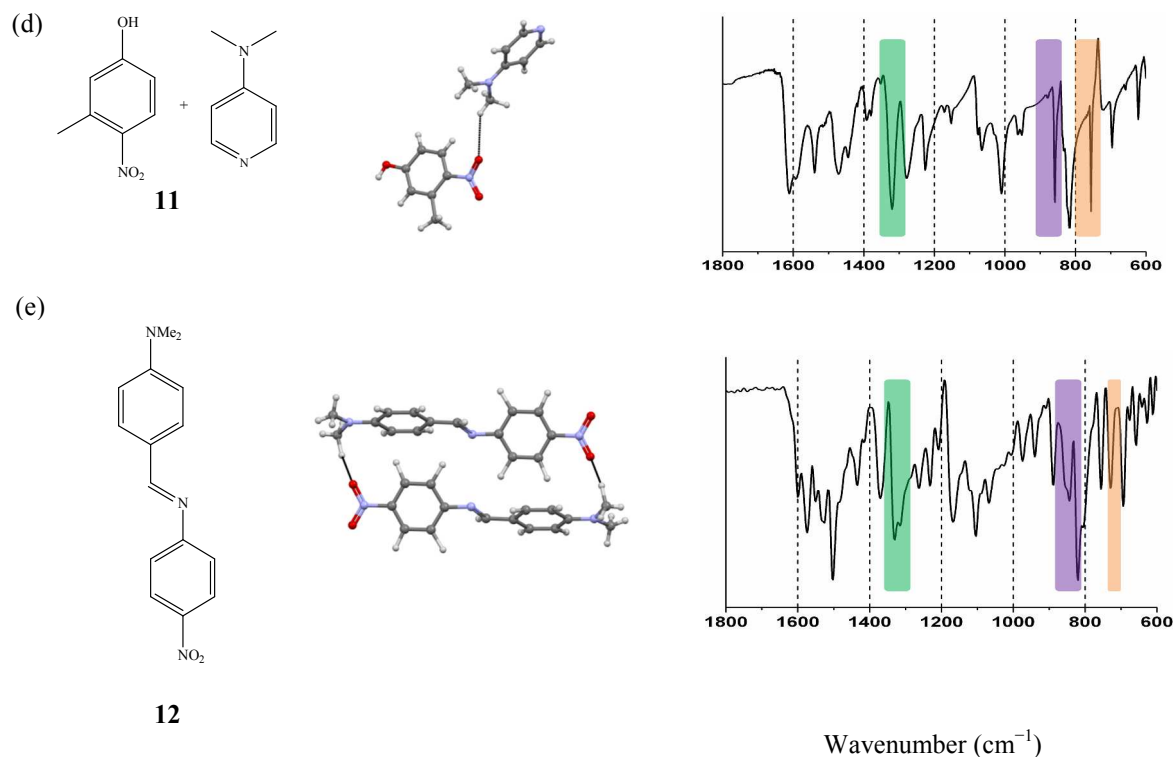


Fig. 4. Compounds (a) **8**, (b) **9**, and (c) **10** with dimer synthon **II** and (d) **11**, (e) **12** with linear $\text{NMe}_2 \cdots \text{O}_2\text{N}$ hydrogen bond and the IR spectra.

Table 3: IR characteristics of compounds **8-12**.

Compounds	Synthon	$\text{NO}_2 \nu_s^A$ band (cm^{-1})	$\text{NO}_2 \nu_s^A$ band shape	δNO_2^B		ωNO_2^C	
			Broad/ Sharp	Position (cm^{-1})	Split (cm^{-1})	Position (cm^{-1})	Split (cm^{-1})
8	Dimer	1334	Broad	827	13	733	13
9	Dimer	1300	Broad	830	10	754	7
10	Dimer	1344	Broad	874	14	718	16
11	Linear	1320	Sharp	858	-	756	-
12	Linear	1330	Sharp	844	-	730	-

^A NO_2 symmetric stretching band, ^B NO_2 scissoring mode, and ^C NO_2 wagging mode.

Compounds **13** and **14** were prepared to determine the synthon in unknown compounds (Fig. 5). The spectra when mapped with the identified markers (Table 12) indicated that both the compounds exhibit the characteristic broad band along with splitting in δNO_2 and ωNO_2 (Table 4) confirming the presence of the $\text{NMe}_2 \cdots \text{O}_2\text{N}$ dimer synthon-**II** in **13** and **14**.

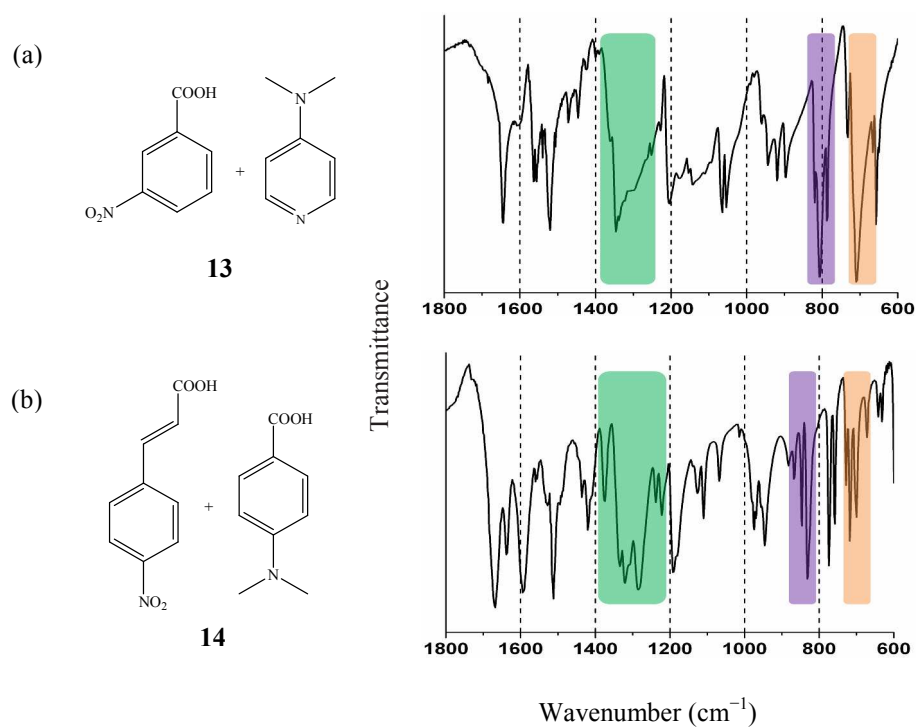


Fig. 5: IR spectra of compounds (a) **13** and (b) **14**.

Table 4: IR characteristics of compounds **13** and **14**.

Compounds	NO ₂ ν _s ^A band (cm ⁻¹)	NO ₂ ν _s ^A band shape	δ NO ₂ ^B		ω NO ₂ ^C		Conclusion
		Broad/ Sharp	Position (cm ⁻¹)	Split (cm ⁻¹)	Position (cm ⁻¹)	Split (cm ⁻¹)	
13	1347	Broad	820	12	732	20	Dimer
14	1334	Broad	846	14	728	10	Dimer

^ANO₂ symmetric stretching band, ^BNO₂ scissoring mode, and ^CNO₂ wagging mode.

To confirm the presence of synthon **II**, the crystal structures of **13** and **14** were determined. The SCXRD confirms the presence of the NMe₂⋯O₂N dimer both in **13** and **14** (Fig. 6).

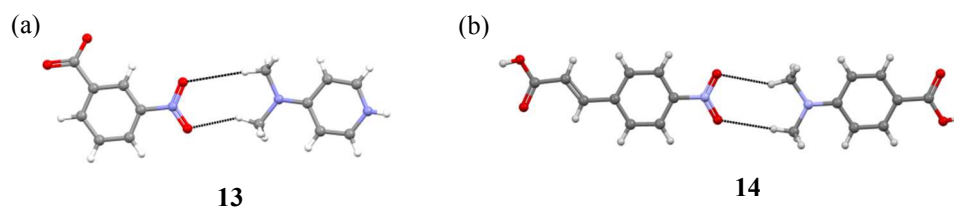


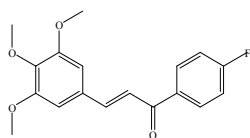
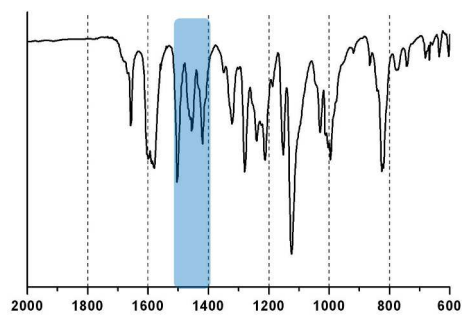
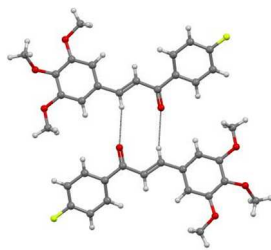
Fig. 6: Crystal structures of compounds (a) **13** and (b) **14**. Both exhibit the dimer synthon **II**.

The C–H···O=C chalcone dimer synthon:

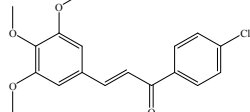
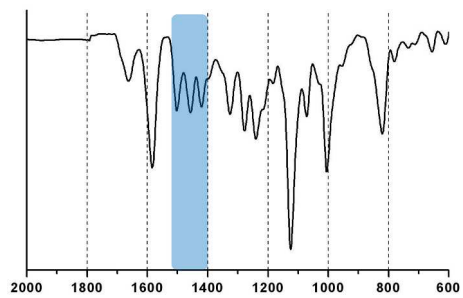
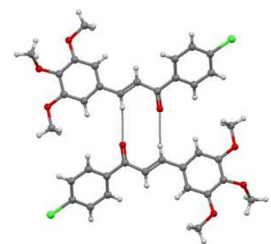
The C–H···O=C hydrogen bond plays a significant role in crystal engineering.³²⁻³⁴ To study the C–H···O=C centrosymmetric dimer synthon (synthon **III**), four chalcones were selected for the identification of marker bands (Fig. 7). The crystal structures of compounds **15-17** and **18-19** are reported, which exhibit dimer (synthon **III**) and linear C–H···O=C hydrogen bond respectively.

In the IR spectrum of a C–H···O=C hydrogen bond, the C=O stretch appears at 1650 cm^{-1} confirming the presence of hydrogen bonded carbonyl.³⁵ This band was seen in the linear as well as C–H···O=C hydrogen bond dimer. However, to identify the dimer of a C–H···O=C hydrogen bond, a characteristic bending absorption was identified for the C–H···O=C hydrogen bond at 1475-1425 cm^{-1} corresponding to torsional (τ) C–H···O deformation of the dimer (Table 5).²⁴ The strong triplet structure of the torsional mode are the marker bands of the synthon **III**. When the O=C from the dimer synthon is bifurcated, further splitting is observed in the triplet marker band (Fig. 7c). Each of the peaks in the C–H···O torsion mode represents a typical C–H···O hydrogen bond. The triplet band structure is absent in case of the linear C–H···O containing compounds (Fig. 7d, 7e).

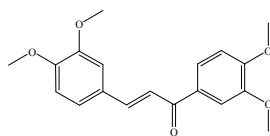
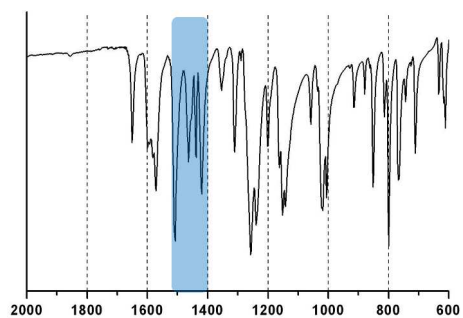
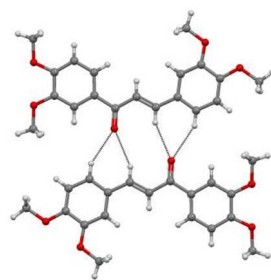
a)

**15**

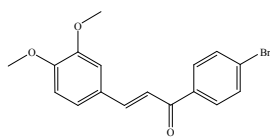
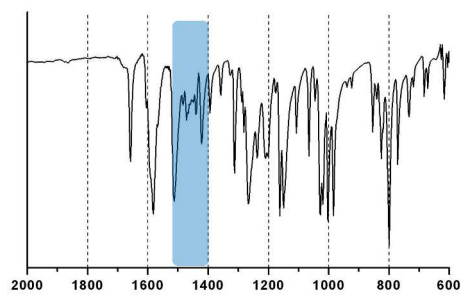
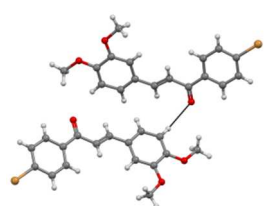
b)

**16**

c)

**17**

d)

**18**

e)

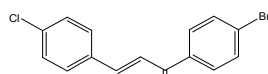
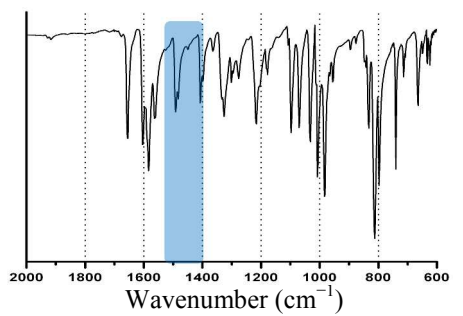
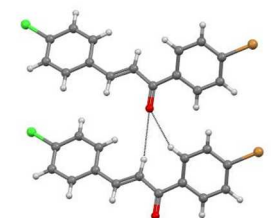
**19**

Fig. 7: Compounds (a) **15**, (b) **16**, and (c) **17** with dimer synthon **III** and (d) **18**, (e) **19** with linear C–H···O=C hydrogen bond and the IR spectra.

Table 5: IR characteristics of compounds **15-19**.

Compounds	Synthon	τ C–H···O (cm ⁻¹)		
		1504	1456	1420
15	Dimer	1504	1456	1420
16	Dimer	1502	1456	1420
17	Dimer	1508	1464	1425, 1420
18	Linear	1512	-	1422
19	Linear	1492	-	1408

Compounds **20** and **21** were prepared to study the synthon structure in unknown powder compounds. The IR spectra were mapped with the markers. It was observed that **20** exhibits the characteristic triplet band structure in the range 1480-1420 cm⁻¹ which is further split indicating the presence of synthon **III** with the bifurcation of O=C in the C–H···O hydrogen bonded dimer (Fig. 8a, Table 6). However, no such triplet band structure was observed in the spectra of **21** confirming the absence of synthon **III** (Fig. 8b).

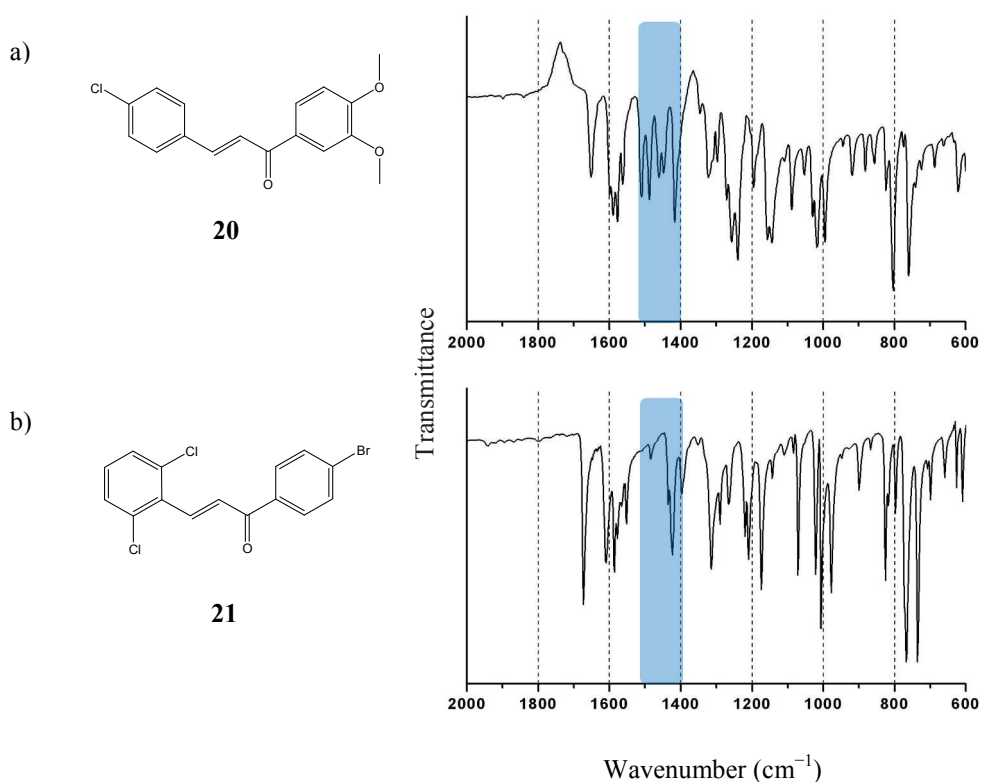
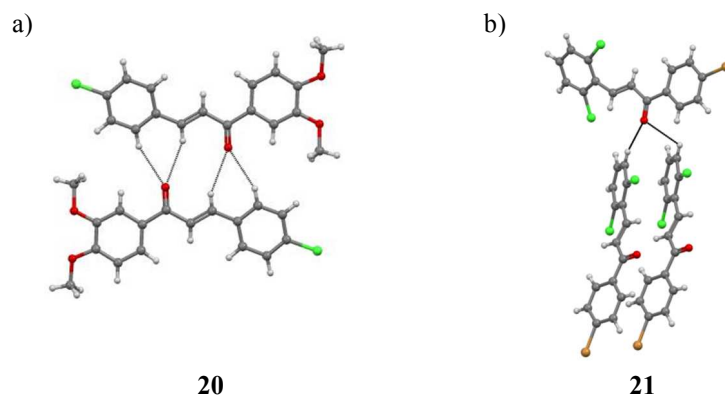


Fig. 8: IR spectrum of compounds (a) **20** and (b) **21** (note the presence and absence of triplet band structure).

Table 6: IR characteristics of compounds **20** and **21**.

Compounds	τ C–H \cdots O (cm ⁻¹)			Conclusion
	1512, 1490	1464, 1450	1418	
20	1512, 1490	1464, 1450	1418	Dimer
21	-	-	1424	Linear

The identification of this synthon was further carried out by SCXRD. The SCXRD confirms the presence of dimer synthon **III** in **20** and absence of dimer in **21** (Fig. 9). Further, the bifurcation of the hydrogen bonded O=C functionality is also observed in **20** validating the reliability of the present process.

**Fig. 9:** Crystal structures of compound (a) **20** (with synthon-**III**) and (b) **21** (with linear C–H \cdots O hydrogen bond).

The C–H \cdots N \equiv C dimer synthon:

Four cyanobenzenes were studied for the identification of marker bands for the C–H \cdots N \equiv C dimer synthon **IV**. The crystal structures of compounds **22-25** are reported, wherein **22-24** exhibit synthon **IV** while **25** is the example of the linear C–H \cdots N \equiv C hydrogen bond (Fig. 10). For all compounds having the dimer C–H \cdots N \equiv C synthon, a split for the C–H stretch is clearly seen in the range 3040-3120 cm⁻¹. Similar splitting of the C–H stretching band was reported for pyrazine dimers which have the C–H \cdots N synthon.²⁵ The occurrence of splitting in the C–H

stretch could be due to Fermi resonance between the strong CH stretching vibrations and C–H bending vibrations of the same symmetry. In the case of the linear C–H \cdots N hydrogen bond for compound **25**, the splitting is absent in the region 3040–3120 cm^{-1} (Table 7).

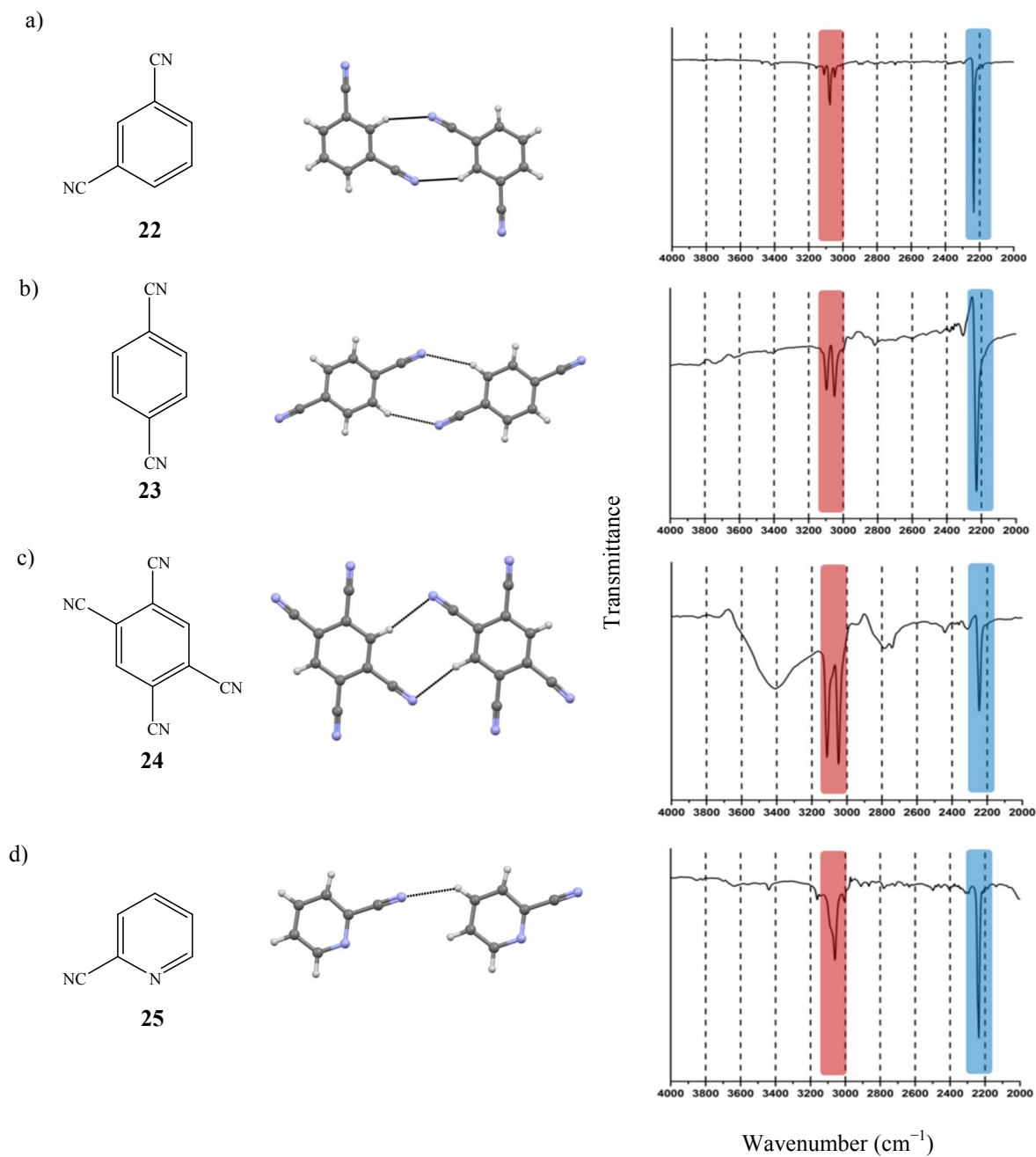
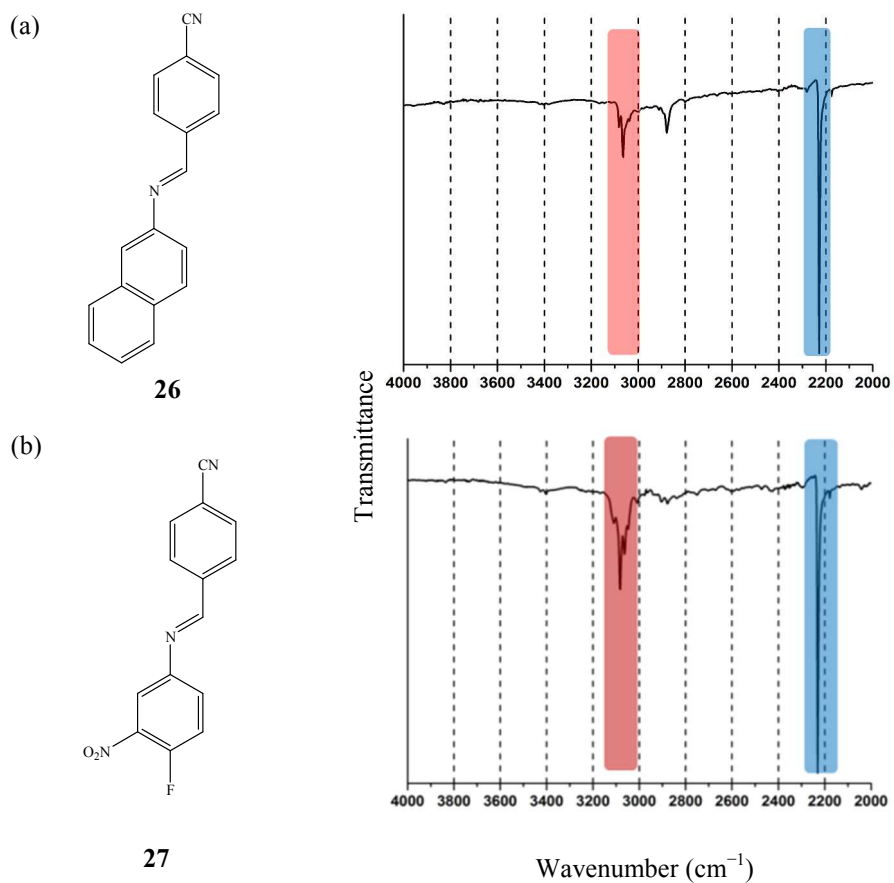


Fig. 10: Compounds (a) **22**, (b) **23**, (c) **24** with dimer synthon-IV and (d) **25** with linear C–H \cdots N \equiv C hydrogen bond and the IR spectra.

Table 7: IR characteristics of compounds 22-25.

Compounds	Synthon	C–H stretch (cm^{-1})	C–H stretch Split (cm^{-1})
22	Dimer	3075, 3050	25
23	Dimer	3096, 3051	45
24	Dimer	3112, 3049	63
25	Linear	3062	–

Compounds **26** and **27** (Fig. 11) were prepared in order to verify the marker bands (Table 12) for this synthon. The IR analysis (Table 8) of both the compounds reveals the spectral characteristic of the linear C–H \cdots N \equiv C synthon.

**Fig. 11:** IR spectrum of compounds (a) **26** and (b) **27**.**Table 8:** IR characteristics of compounds 26-27.

Compounds	C–H stretch (cm^{-1})	C–H stretch Split (cm^{-1})	Conclusion
26	3064	–	Linear
27	3062	–	Linear

Further SCXRD supports the IR analysis for compound **27** (Fig. 12). The quality of the single crystals of compound **26** was too poor to diffract. However, the IR analysis indicates the absence of dimer synthon **IV** (Table 8).

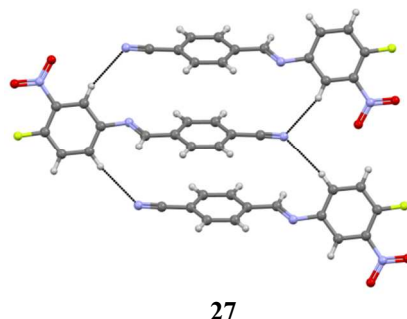


Fig. 12: Crystal structure of compound **27** with linear C–H···N≡C hydrogen bond.

The single point and bifurcated C–H···F–C synthon:

For the study of the C–H···F hydrogen bond, five compounds **28-32** were selected (Fig. 13). The crystal structures of the compounds are constituted with carboxylic acid dimers. Three different types of C–H···F hydrogen bond patterns were observed in these compounds. For **28-29** there is no bifurcation of either C–H or fluorine bonded interactions, in **30** there is a bifurcation of hydrogen bond from fluorine whereas in **31-32** both C–H and fluorine are involved in bifurcated hydrogen bonds. This is reflected in the IR spectra in the δ C–H···F vibration of the compounds.³⁶ Characteristic marker bands of the δ C–H···F hydrogen bond are observed in the range 1330-1280 cm^{-1} . It can be seen from the shifts that the δ C–H···F vibration (in plane bending) frequency increases (blue shift) with the number of bifurcations. This is expected as an increase in the number of bifurcations draws out electrons from the C–H bond and this causes the deformation band to blue shift (Table 9).

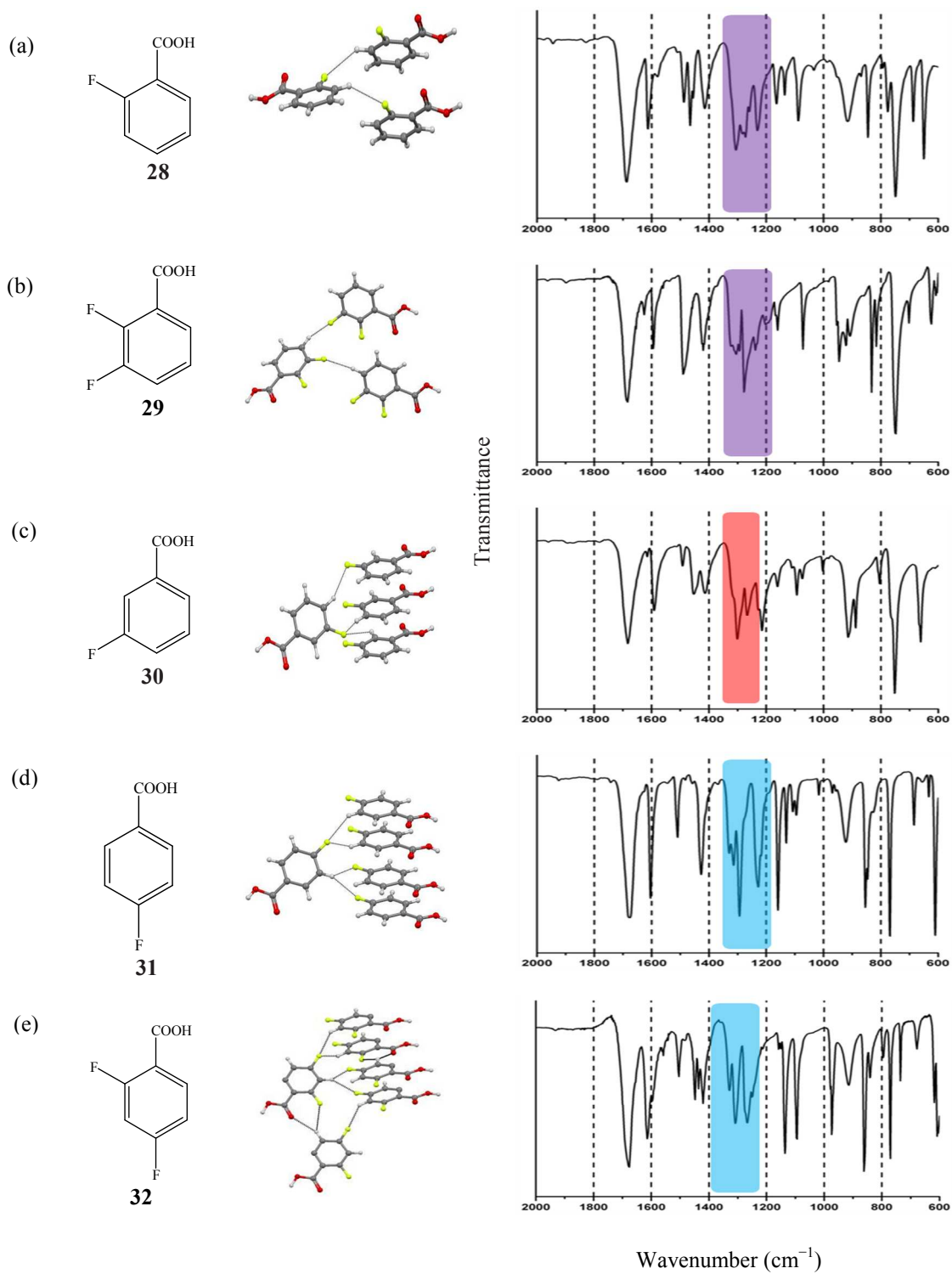
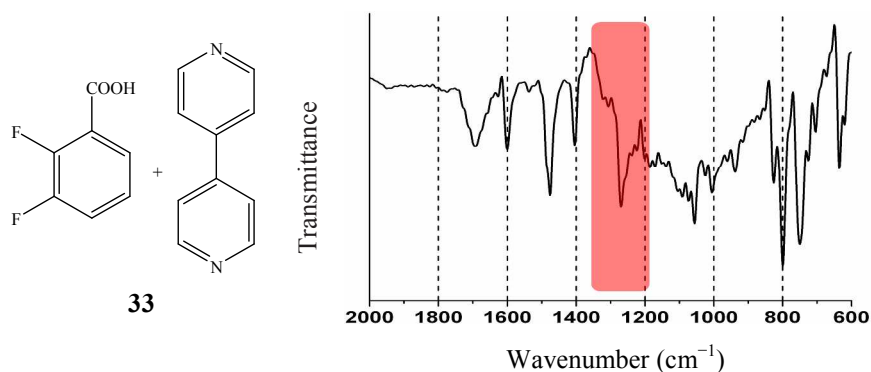


Fig. 13: Compounds (a) 28, (b) 29, (c) 38, (d) 31, and (e) 32 and the IR spectra.

Table 9: IR characteristics of compounds 28-32.

Compounds	Type of C–H interaction	Type of F interaction	δ C–H...F (cm^{-1})
28	Non-bifurcated	Non-bifurcated	1308, 1271, 1230
29	Non-bifurcated	Non-bifurcated	1305, 1278, 1238
30	Non-bifurcated	Bifurcated	1318, 1300, 1268
31	Bifurcated	Bifurcated	1330, 1310, 1290
32	Bifurcated	Bifurcated	1330, 1312, 1270

Compound 33 was studied as unknown system (Fig. 14). IR spectrum investigation suggests non-bifurcation in C–H interaction and bifurcation in C–F...H–C hydrogen bond (Table 10).

**Fig.14:** IR spectrum of 33.

SCXRD analysis finally confirms the IR conclusion (Fig. 15). This example shows how adequately the IR pattern changes on different synthon formation by the same compound; 2,3-difluorobenzoic acid and its cocrystal.

Table 10: IR characteristics of compound 33.

Compounds	δ C–H...F (cm^{-1})	Conclusion	
		Type of C–H interaction	Type of F interaction
33	1322, 1306, 1270	Non-bifurcated	Bifurcated

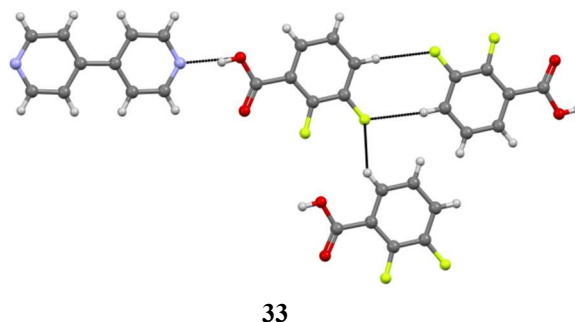


Fig.15: Crystal structure of compound **33**, exhibit non-bifurcation in C–H···F and bifurcation in C–F···H–C hydrogen bond.

The N–H··· π synthon:

Among the weaker intermolecular interactions, the N–H··· π interaction seems to be less investigated.³⁷ We have employed IR to look at the vibration bands of the –NH₂ functional group involved in synthon formation. The reported compounds **34–38** (Fig. 16) are selected to study the presence of the N–H··· π synthon. Among these, **34–36** have the synthon **VI** while **37** and **38** exhibit N–H···Cl and N–H···N hydrogen bond, respectively. The spectral analysis of **34** shows a split in NH₂ deformation mode at ~1610 cm⁻¹ which is also seen for compounds **35** and **36** (Table 11). This split is absent in **37–38** and appears as a single absorption band at 1614 and 1630 cm⁻¹, respectively. The splitting is due to the asymmetry induced by the N–H··· π interaction.

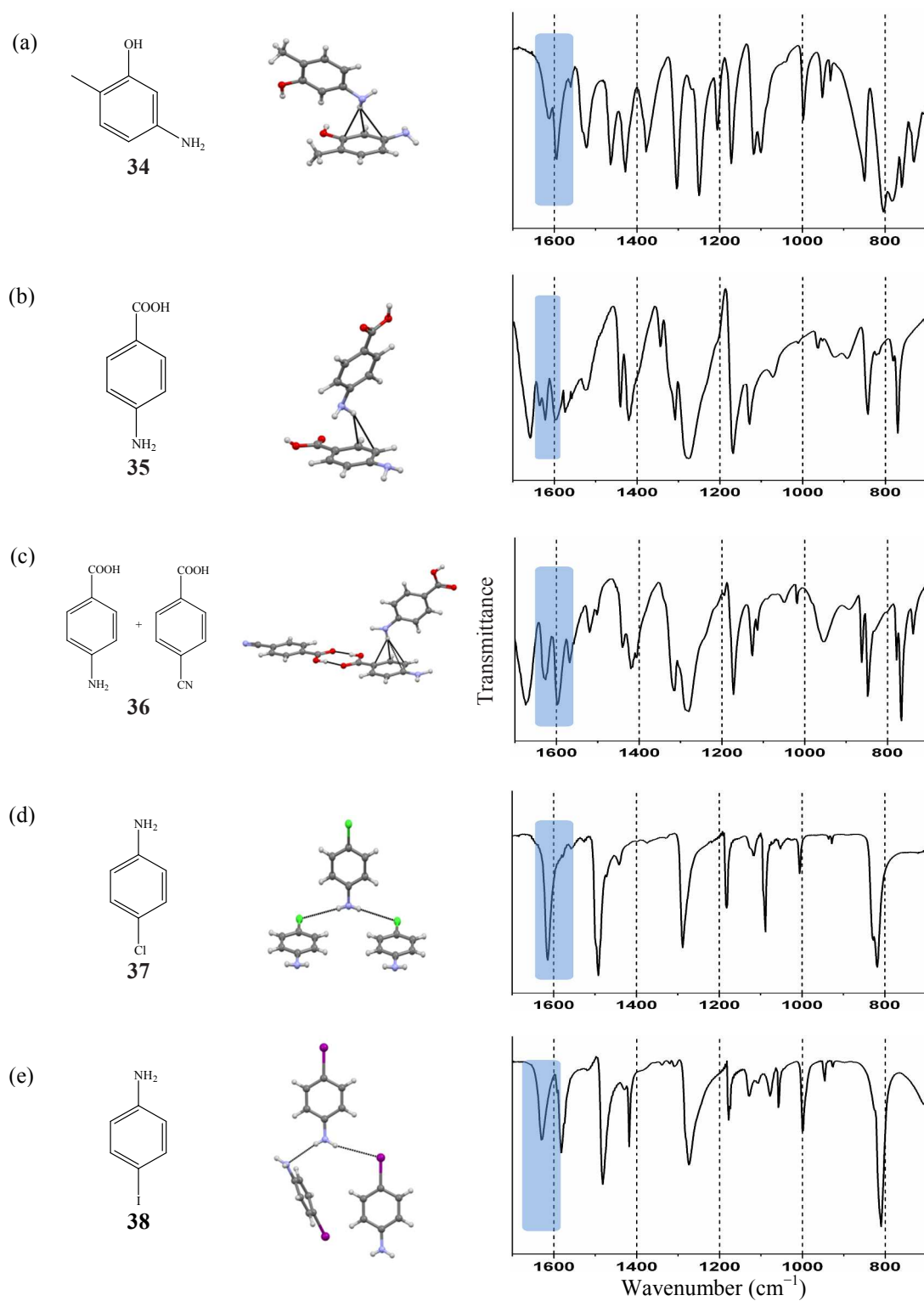


Fig. 16: Compounds (a) **34**, (b) **35**, and (c) **36** with synthon **VI** and (d) **37**, (e) **38** without N–H··· π synthon and the IR of the respective compounds.

Table 11: IR characteristics of compounds **34-38**.

Compounds	Synthon	NH ₂ deformation (cm ⁻¹)	
		Position	Split
34	N-H...π	1612	18
35	N-H...π	1636	14
36	N-H...π	1624	25
37	N-H...Cl	1614	-
38	N-H...N N-H...I	1630	-

Compound **39** was used to identify the synthon in unknown system (Fig. 17). The IR analysis clearly indicates the presence of N-H...π synthon in **39** (Table 12). However, the poor quality of the crystals resisted the crystal structure determination.

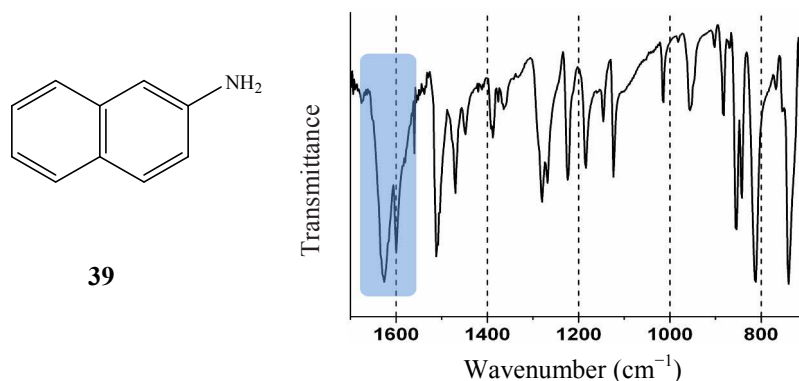


Fig.17: IR spectra of **39**.

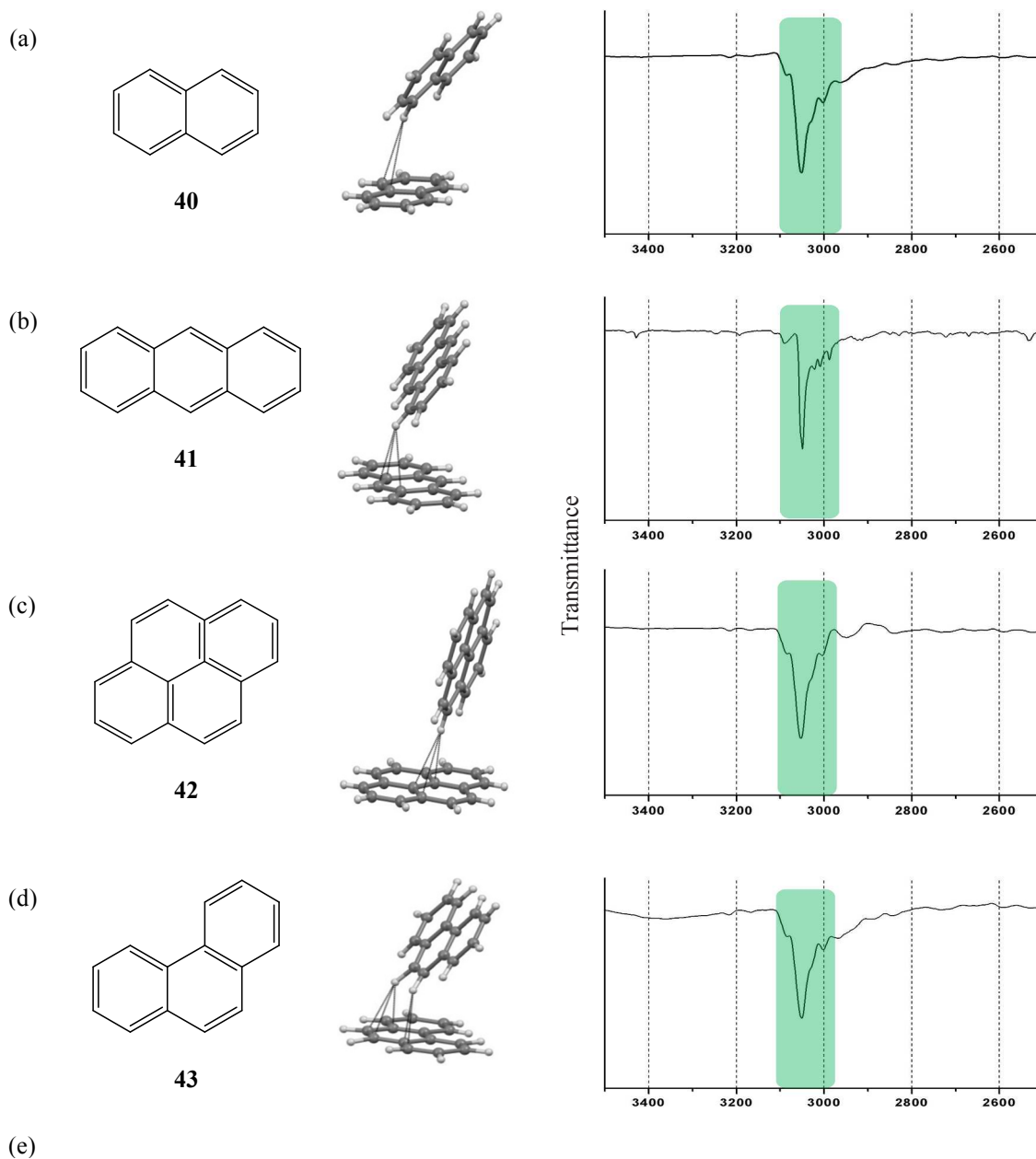
Table 12: IR characteristics of compound **39**.

Compounds	NH ₂ deformation (cm ⁻¹)		Conclusion
	Position	Split	
39	1626	26	N-H...π synthon

The C-H...π synthon:

The C-H...π interaction is a weak attractive interaction between the C-H bond and the π electron cloud.³⁸ It is ubiquitous in π-conjugated systems. In this study, naphthalene (**40**), anthracene (**41**), pyrene (**42**), phenanthrene (**43**), 1,4-dibromobenzene (**44**) and 1,4-dichlorobenzene (**45**) were

selected. Compounds **40-43** exhibit C–H $\cdots\pi$ interactions extensively whereas **44** and **45** involve the C–H \cdots Br and C–H \cdots Cl hydrogen bond, respectively. A broad band is identified in the range 3500–2700 cm^{-1} (Fig. 18). The IR active C–H stretch shows remarkable similarity in the four compounds with the broad band showing substructure peaks at ~ 3050 cm^{-1} (Table 13). However, in **44** and **45** this broad band shape is shifted to a sharp peak at ~ 3080 cm^{-1} .



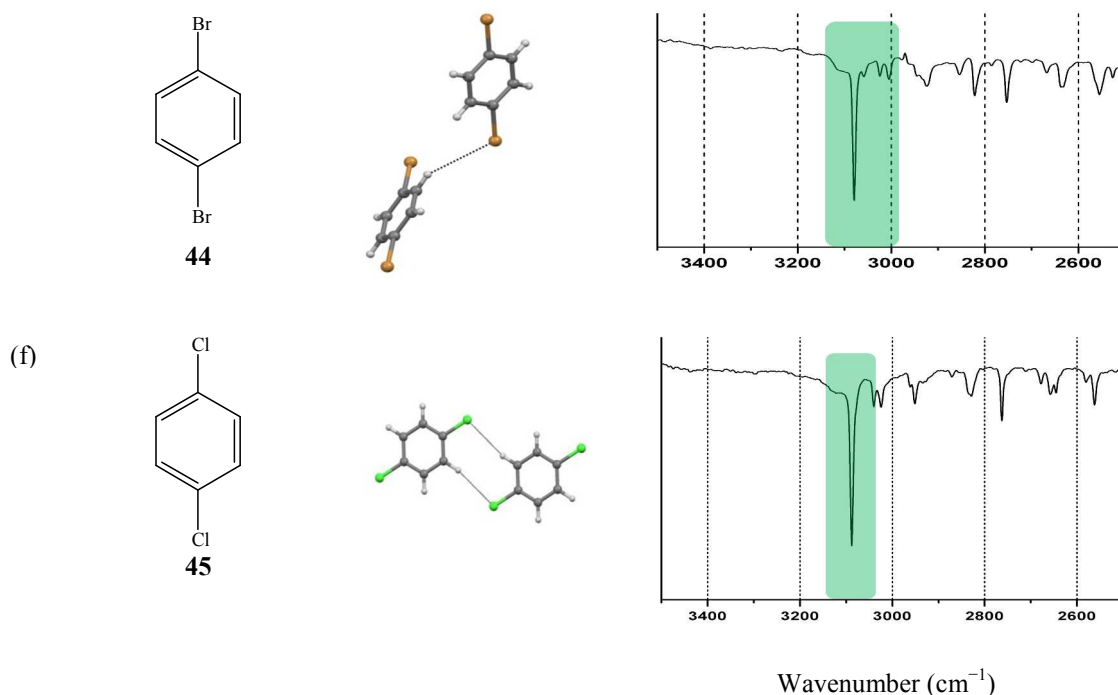


Fig. 18: Compounds (a) **40**, (b) **41**, (c) **42** and (d) **43** with synthon **VII** and (e) **44**, (f) **45** (does not have C–H $\cdots\pi$ synthon) and the IR spectra.

Table 13: IR characteristics of compounds **40-45**.

Compounds	Synthon	C–H stretch (cm^{-1})
40	C–H $\cdots\pi$	3052
41	C–H $\cdots\pi$	3050
42	C–H $\cdots\pi$	3052
43	C–H $\cdots\pi$	3052
44	C–H $\cdots\text{Br}$	3080
45	C–H $\cdots\text{Cl}$	3088

The identified IR band pattern was used to recognize the presence or absence of the synthon in **46** (Fig. 19). IR study (Table 14) suggests the presence of C–H $\cdots\pi$ in **46** which was further confirmed by SCXRD (Fig. 20).

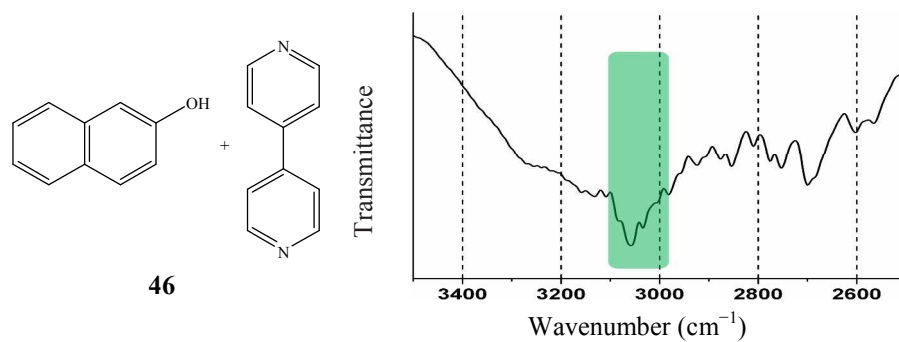


Fig.19: IR spectra of 46.

Table 14: IR characteristics of compound 46.

Compounds	C-H stretch (cm^{-1})	Conclusion
46	3056	C-H $\cdots\pi$

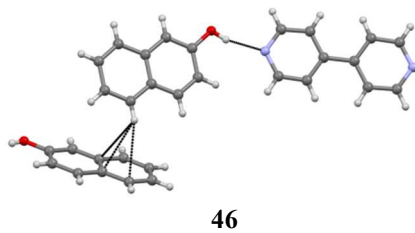
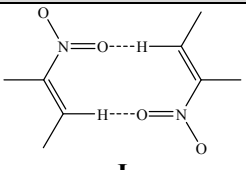
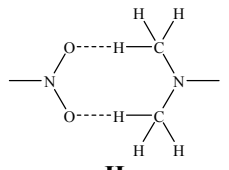
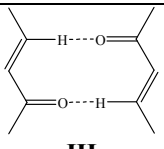
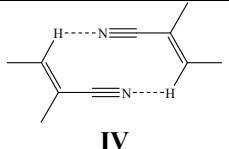
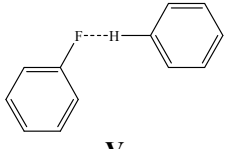
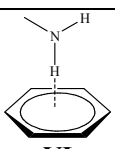
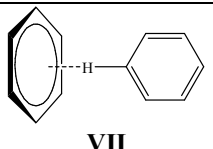


Fig.20: Crystal structure of compound 46, exhibit the C-H $\cdots\pi$ synthon.

Table 15: List of IR characteristics of synthons in this study.

Synthon	IR band assignment	Characteristics
 <p style="text-align: center;">I</p>	$\sim 1350 \text{ cm}^{-1}$: $\nu_s \text{ NO}_2$	(1) $I_{as} \leq I_s$ (2) Split band
 <p style="text-align: center;">II</p>	$\sim 1350 \text{ cm}^{-1}$: $\nu_s \text{ NO}_2$	(1) Broad band
	$\sim 840 \text{ cm}^{-1}$: $\delta \text{ NO}_2$	(2) Split band
	$\sim 730 \text{ cm}^{-1}$: $\omega \text{ NO}_2$	(3) Split band
 <p style="text-align: center;">III</p>	$\sim 1520\text{-}1410 \text{ cm}^{-1}$: $\delta \text{ C-H}\cdots\text{O}$	(1) Triplet band
 <p style="text-align: center;">IV</p>	$\sim 3050 \text{ cm}^{-1}$: C-H stretch	(1) Split band
 <p style="text-align: center;">V</p>	$\sim 1308 \text{ cm}^{-1}$: $\delta \text{ C-H}\cdots\text{F}$	(1) Frequency of C-H...F
	$\sim 1318 \text{ cm}^{-1}$: $\delta \text{ C-H}\cdots\text{F}$	(2) Frequency of C-H...F
	$\sim 1330 \text{ cm}^{-1}$: $\delta \text{ C-H}\cdots\text{F}$	(3) Frequency of C-H...F
 <p style="text-align: center;">VI</p>	$\sim 1610 \text{ cm}^{-1}$: N-H deformation mode	(1) Split band
 <p style="text-align: center;">VII</p>	$\sim 3000 \text{ cm}^{-1}$: C-H stretch	(1) Identical band structure

Conclusions

A five step IR spectroscopic method has been developed to identify weakly hydrogen bonded dimer synthons. Comparison of the IR spectra of the dimer with the linear hydrogen bond of the same functional groups from similar compounds reveals characteristic differences in the C–H stretching and bending modes, which are termed as marker bands. The marker bands were further tested in compounds whose crystal structures were not known and the method is found to be promising in identifying supramolecular synthons involved in the polycrystalline/powder materials. An IR band-shape study of C–H \cdots π and N–H \cdots π synthons can be comparatively complicated but the present method provides a simple alternative for predicting the presence of C–H \cdots π and N–H \cdots π synthons. The present synthon IR analysis is also flexible enough to apply for polymorphs, cocrystals, salts and can be used in presence of different functional groups other than those involved in synthon formation. This simple and rapid study will be helpful for systems involving weak hydrogen bonds where SCXRD methods are difficult.

Experimental:

Compounds **6**, **20**, **21**, **26**, and **27** were synthesized according to reported procedure (supplementary information S1).³⁹

Crystallization:

Compound 6: The compound was crystallized from MeOH.

Compound 7: **6** was dissolved in MeOH and allowed to stand for slow evaporation of the solvent. Good quality crystals suitable for SCXRD were obtained after 4 days.

Compound 13: 3-Nitrobenzoic acid and 4-Dimethylaminopyridine were taken in 1:1 molar ratio in a mortar and ground with few drops of MeOH for 5 minutes. The powder mixture was used for IR spectra recording (for PXRD see supplementary information S2). The ground mixture was then dissolved in different solvents. Crystals were obtained from MeOH after 3 days. Melting point: 162 °C.

Compound 14: 4-Nitrocinnamic acid and 4-dimethylaminobenzoic acid were taken in 1:1 molar ratio in a mortar and ground with few drops of MeOH for 5 minutes. Formation of coloured mixture due to charge transfer confirms the formation of cocrystal. The powder mixture was used for IR analysis (for PXRD see supplementary information S2). Melting point: 243 °C.

Compound 20: The compound was crystallized from acetone.

Compound 21: The compound was crystallized from acetone.

Compound 27: The compound was crystallized from MeOH.

Compound 33: 2,3-Difluorobenzoic acid and 4,4'-bipyridine were taken in 2:1 molar ratio in a mortar and ground with few drops of MeOH for 5 minutes. The powder mixture was used for IR spectra recording (for PXRD see supplementary information S2). The ground mixture was then

dissolved in different solvents. Crystals were obtained by slow evaporation of THF solution of the compound after 4 days. Melting point: 143 °C.

Compound 46: β -Naphthol and 4,4'-bipyridine were taken in 2:1 molar ratio in a mortar and ground with few drops of MeOH for 5 minutes. The powder mixture was used for IR spectra recording (for PXRD see supplementary information S2). The ground mixture was then dissolved in different solvents. Crystals were obtained by slow evaporation of MeOH solution of the compound after 4 days. Melting point: 92 °C.

Melting point

The melting points of the compounds were measured on an automated Büchi M-560 melting point apparatus, using glass capillaries (for melting points see supplementary information S1).

Single crystal X-ray diffraction

SCXRD data were collected on a Rigaku Mercury 375R/M CCD (XtaLAB mini) diffractometer using graphite monochromatic Mo K α radiation, with a Rigaku low temperature gas spray cooler facility. Data were processed with the Rigaku *CrystalClear 2.0* software^{40,41}. Structure solution and refinements were performed using SHELX97⁴² implemented in the WinGXsuite⁴³. The references of the known crystal structures are given in the supporting information. The crystallographic data is given in the supplementary information for the newly obtained crystal structures (section S3).

FTIR spectroscopy

Solid state IR spectra of the compounds were recorded on a Perkin Elmer frontier infrared spectrometer in ATR mode using diamond crystal as an ATR sampler from 4000-600 cm^{-1} with a resolution of $\pm 2 \text{ cm}^{-1}$. Complete solid state IR spectra of all compounds are given in the supplementary information, S4.

Acknowledgements

S.S. and M.K.M. are grateful to the CSIR for a Senior Research Fellowship. L.R. and S.J. thanks the DST for a Young Scientist Fellowship. S.G. is grateful to IISc Bangalore for a fellowship. G.R.D. thanks the DST for a J. C. Bose Fellowship.

References:

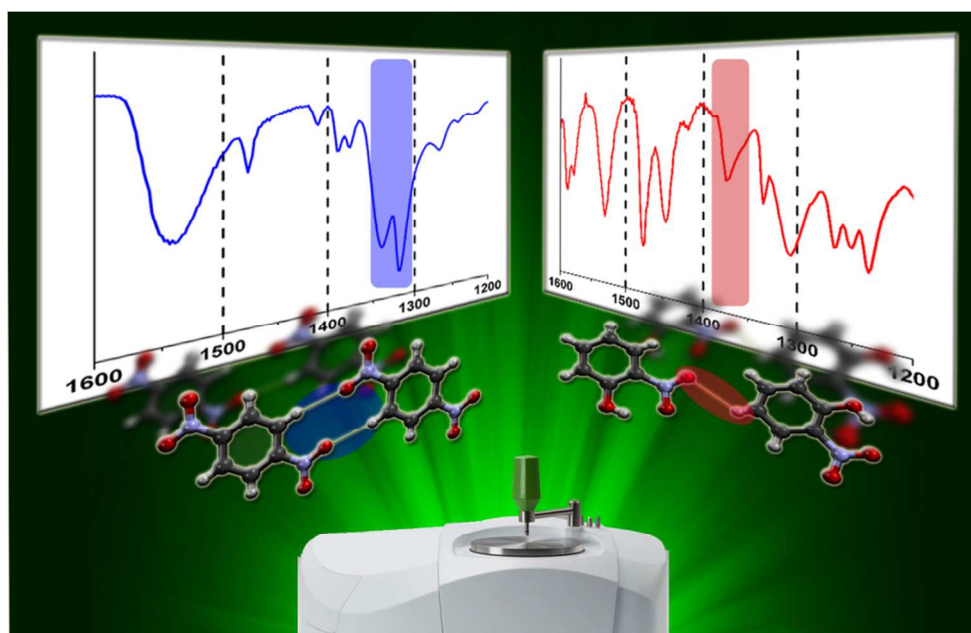
- 1 G. R. Desiraju, *Crystal Engineering: The Design of Organic Solids*, Elsevier: Amsterdam, 1989, 175–198.
- 2 (a) G. R. Desiraju, *Angew.Chem., Int. Ed.*, 1995, **34**, 2311–2327; (b) G. R. Desiraju, *Angew. Chem., Int. Ed.*, 2007, **46**, 8342–8356; (c) G. R. Desiraju, *Chem. Commun.*, 2005, 2995–3001; (d) P. Vishweshwar, R. Thaimattam, M. Jaskolski and G. R. Desiraju, *Chem. Commun.*, 2002, 1830–1831.
- 3 *Pharmaceutical Salts and Co-crystals*, ed. J. Wouters and L. Quere, Royal Society of Chemistry, 2011.
- 4 Ö. Almarsson and M. J. Zaworotko, *Chem. Commun.*, 2004, 1889–1896.
- 5 C. P. Price, A. L. Grzesiak and A. J. Matzger, *J. Am. Chem. Soc.*, 2005, **127**, 5512–5517.
- 6 M. R. Caira, *Mol. Pharmacol.*, 2007, **4**, 310–316.
- 7 N. J. Babu and A. Nangia, *Cryst. Growth Des.*, 2011, **11**, 2662–2679.
- 8 A. V. Trask and W. Jones, *Top. Curr. Chem.*, 2005, **254**, 41–70.
- 9 J. D. Dunitz and W. B. Schweizer, *Chem. Eur. J.*, 2006, **12**, 6804–6815.
- 10 G. R. Desiraju and T. Steiner, *The Weak Hydrogen Bond in Structural Chemistry and Biology*, Oxford University Press, Oxford, 1999.
- 11 G. R. Desiraju, *Nature*, 2001, **412**, 397–400.
- 12 (a) G. R. Desiraju, *Acc. Chem. Res.*, 1996, **29**, 441–449; (b) S. S. Kuduva, D. C. Craig, A. Nangia and G. R. Desiraju, *J. Am. Chem. Soc.*, 1999, **121**, 1936–1944; (c) A. Nangia and G.

- R. Desiraju, *J. Mol. Str.*, 1999, **474**, 65–79; (d) R. Thaimattam, P. J. Langley, J. Hulliger and G. R. Desiraju, *New J. Chem.*, 1998, 1307–1309; (e) G. R. Desiraju, B. N. Murty and K. V. R. Kishan, *Chem. Mater.*, 1990, **2**, 447–449.
- 13 (a) A. Nangia and G. R. Desiraju, *Top. Curr. Chem.*, 1998, **198**, 57–95; (b) J. D. Dunitz, *Pure Appl. Chem.*, 1991, **63**, 177–185; (c) S. Paliwal, S. Geib and C. S. Wilcox. *J. Am. Chem. Soc.*, 1994, **116**, 4497–4498; (d) C. A. Hunter. *Chem. Soc. Rev.*, 1994, **23**, 101–109; (e) C. V. K. M. Sharma, K. Panneerselvam, T. Pilati and G. R. Desiraju, *J. Chem. Soc., Chem. Commun.*, 1992, 832–833.
- 14 (a) H. L. Anderson, A. Bashall, K. Henrick, M. McPartlin and J. K. M. Sanders, *Angew. Chem.*, 1994, **106**, 445–447; (b) F. Vögtle, W. M. Müller, U. Müller, M. Bauer and K. Rissanen, *Angew. Chem.*, 1993, **105**, 1356–1358; (c) E. C. Constable, A. J. Edwards, P. R. Raithby and J. V. Walker. *Angew. Chem.*, 1993, **105**, 1486–1487; (d) C. Dietrich-Buchecker, B. Frommberger, I. Luer, J.-P. Sauvage and F. Vögtle; *Angew. Chem.*, 1993, **105**, 1526–1529; (e) S. S. Pathaneni and G. R. Desiraju, *Dalton Trans.*, 1993, 2505–2508; (f) P. R. Ashton., D. Philp, N. Spencer, J. F. Stoddart and D. J. Williams, *J. Chem. Soc. Chem. Commun.*, 1994, 181–184; (g) F. A. Wintner, M. M. Conn and J. Jr. Rebek, *Acc. Chem. Res.*, 1994, **27**, 198–203; (h) M. J. Gunter, D. C. R. Hockless, M. R. Johnston, B. W. Skelton and A. H. White, *J. Am. Chem. Soc.*, 1994, **116**, 4810–4823; (i) T. S. Thakur, M. T. Kirchner, D. Bläser, R. Boese and G. R. Desiraju, *CrystEngComm*, 2010, **12**, 2079–2085.
- 15 (a) M. D. Hollingsworth and M. D. Ward, *Chem. Mater.*, 1994, **6**, 1087–1462, (b) J. C. MacDonald and G. M. Whitesides, *Chem. Rev.* 1994, **94**, 2383–2420.
- 16 (a) S. Ghosh, A. Mondal, M. S. R. N. Kiran, U. Ramamurty, and C. M. Reddy, *Cryst. Growth Des.*, 2013, **13**, 4435–4441; (b) L. Keszthelyi, *Orig. Life*, 1981, **11**, 9–21; (c) I. C. Lin and U.

- Rothlisberger, *Phys. Chem. Chem. Phys.*, 2008, **10**, 2730–2734; (d) D. Ž. Veljković, V. B. Medaković, J. M. Andrić and S. D. Zarić, *CrystEngComm*, 2014, DOI: 10.1039/C4CE00595C; (e) S. Sarkhel and G. R. Desiraju, *Proteins: Structure, Function and Bioinformatics*, 2004, **54**, 247–259.
- 17 S. L. Price, *Acc. Chem. Res.*, 2009, **42**, 117–126.
- 18 G. M. Day, W. D. S. Motherwell, H. L. Ammon, S. X. M. Boerrigter, R. G. Della Valle, E. Venuti, A. Dzyabchenko, J. D. Dunitz, B. Schweizer, B. P. van Eijck, P. Erk, J. C. Facelli, V. E. Bazterra, M. B. Ferraro, D. W. M. Hofmann, F. J. J. Leusen, C. Liang, C. C. Pantelides, P. G. Karamertzanis, S. L. Price, T. C. Lewis, H. Nowell, A. Torrisi, H. A. Scheraga, Y. A. Arnautova, M. U. Schmidt and P. Verwer, *Acta Crystallogr., Sect. B: Struct. Sci.*, 2005, **61**, 511–527.
- 19 J. A. R. P. Sarma and G. R. Desiraju, *Cryst. Growth Des.*, 2002, **2**, 93–100.
- 20 (a) A. Mukherjee, S. Tothadi, S. Chakraborty, S. Ganguly and G. R. Desiraju, *CrystEngComm*, 2013, **15**, 4640–4654. (b) S. Saha, S. Ganguly and G. R. Desiraju, *Aust. J. Chem.*, 2014, doi.org/10.1071/CH14361.
- 21 (a) H. G. Brittain, *Cryst. Growth Des.*, 2011, **11**, 2500–2509; (b) H. G. Brittain, *Chirality*, 2013, **25**, 8–15.
- 22 G. S. Denisov, J. Mavri and L. Sobczyk, *Hydrogen bonding-new insights*, ed. S. J. Grabowski, Springer, 2006, 377–416.
- 23 J. Antony, G. von Helden, G. Meijer and B. Schmidt, *J. Chem. Phys.*, 2005, **123**, 014305.
- 24 B. I. Stefanov, Z. Topalian, C. G. Granqvist and L. Osterlund, *J. Mol. Catal. A: Chem.*, 2014, **381**, 77–88.

- 25 M. Busker, Y. N. Svartsov, T. Häber and K. Kleinermanns, *Chem. Phys. Lett.*, 2009, **467**, 255–259.
- 26 M. Samsonowicz, R. S'Wislocka, E. Regulska and W. Lewandowski, *Int. J. Quantum Chem.*, 2007, **107**, 480–494.
- 27 S. X. Raja, A. William and S. Gunasekaran, *Proc. Indian Natl. Sci. Acad.*, 1993, **59A**, 215–220.
- 28 E. B. Burgina, V. P. Baltakhinov, E.V. Boldyreva, E.S. Stoyanov, N. Y. Zhanpeisov and G. M. Zhidomirov, *J Mol. Struct.*, 1993, **296**, 53–59.
- 29 L. J. Bellamy, *Advances in Infrared Group frequencies*, Methuen and company, London, 1968.
- 30 J. Dreyer, *J. Chem. Phys.*, 2005, **122**, 184306.
- 31 C. K. Nandi, M. K. Hazra and T. Chakraborty, *J. Chem. Phys.*, 2005, **123**, 124310.
- 32 A. I. Kitaigorodskii, *Molecular Crystals and Molecules*, Academic Press, New York, 1973.
- 33 K. Biradha, C. V. K. Sharma, K. Pnnneerselvam, L. Shimoni, H. L. Carrell, D. E. Zacharias and G. R. Desiraju, *J. Chem. Soc. Chem. Commun.*, 1993, 1473–1475.
- 34 C. Nakamura, N. Kawasaki, H. Miyataka, E. Jayachandran, I. H. Kim, K. L. Kirk, T. Taguchi, Y. Takeuchi, H. Horie and T. Satoh, *Bioorg. Med. Chem.*, 2002, **10**, 699–706.
- 35 P. J. A. Ribeiro-Claro, M. G.B. Drew and V. Félix, *Chem. Phys. Lett.*, 2002, **356**, 318–324.
- 36 (a) A. J. Barnes, H. E. Hallam, J. D. R. Howells and G. F. Scrimshaw, *J. Chem. Soc., Faraday Trans., 2*, 1973, **69**, 738–749. (b) E. Kryachko and S. Scheiner, *J. Phys. Chem. A*, 2004, **108**, 2527–2535.

- 37 P. Ottiger, C. Pfaffen, R. Leistand, S. Leutwyler, R. A. Bachorz and W. Kloppe, *J. Phys. Chem. B*, 2009, **113**, 2937–2943.
- 38 M. Nishio, *CrystEngComm*, 2004, **6**, 130–158.
- 39 J. L. Wardell, J. N. Low, J. M. S. Skakle and C. Glidewell, *Acta Crystallogr., Sect. B: Struct. Sci.*, 2006, **62**, 931–943.
- 40 Crystal Clear 2.0 (Rigaku Corporation: Tokyo).
- 41 J. Pflugrath, *Acta Crystallogr., Sect. D: Biol. Crystallogr.*, 1999, **55**, 1718–1725.
- 42 G. M. Sheldrick, SHELX-97: Program for the Solution and Refinement of Crystal Structures 1997 (University of Göttingen: Göttingen).
- 43 L. J. Farrugia, *J. Appl. Crystallogr.*, 1999, **32**, 837–838.

TOC:

We describe a five step IR spectroscopic method that identifies supramolecular synthons in weak hydrogen bonded dimer assemblies, bifurcated systems, and π -electron mediated synthons.